Direct Deposition of Au Nanoparticles onto TiO_2 Rods

Jaykrushna Das, Gayatri Rane, and Deepa Khushalani*
Materials Chemistry Group, Department of Chemical Sciences, Tata Institute of Fundamental Research, Mumbai 400005, India

(Received April 28, 2009; CL-090423; E-mail: khushalani@tifr.res.in)

A novel nongrafting route has been developed to anchor Au nanoparticles (NPs) onto titanium oxide rods. These rods have been synthesized through a process involving a glycolate precursor. A facile solid-state transformation allows anatase and rutile phases to be formed *without* the overall rod-like morphology being altered. Importantly, the sizes of the rods can be controlled through varying reflux time and temperature only, and hence the procedure does not necessitate the use of additives. These rods have then been used as supports to deposit Au NPs through a simple method that relies on hydrophobic interactions.

Titanium oxide is one of the most versatile wide band gap semiconductors, and it is used in a variety of applications such as photovoltaics and catalysis.[1] Specifically, one-dimensional structures of metal oxides (i.e., tubes or rods) on the micrometer to nanometer length scale have shown improved performance over their bulk analogues, especially for dye-sensitized solar cell applications.[2–5] For preparation of TiO_2, most synthetic routes commonly rely on commercially available precursors such as titanium salts, tetrahalides, or alkoxides. These reagents, however, are highly moisture sensitive. It becomes difficult to control the rates of hydrolysis and condensation reactions, and this inevitably leads to formation of polydispersed TiO_2 structures where the overall morphology cannot be easily controlled. Moreover, fabrication of composite materials that consist of titanium oxide with metal nanoparticles (NPs) grafted onto the surface has gained considerable momentum in recent years mainly because the band gap and optical properties can be tuned depending on the amount of loading of metal NPs.[6,7] To date these composite materials have been synthesized via a multistep process. First the surface of the oxide is functionalized by converting the surface hydroxy groups to either amines or thiols. Subsequently, the metal NPs are reacted with these $-NH_2$ or $-SH$ moieties such that the NPs are then covalently anchored to the surface.[8] The functionalization of metal oxide is not only a time-consuming process but also, sometimes, the materials degrade and loose their structural integrity during this nontrivial process. In this report, a relatively temperate process is presented which provides (1) rods of titanium oxide that can be altered in sizes and (2) a route for a novel nongrafting process to deposit Au NPs on the surface of these rods.

The details of the synthesis can be obtained from Supporting Information. Figure 1 shows the data from diffraction studies performed after heating the product from RT up to 900 °C. The as-synthesized titanium glycolate precursor maintains its structure up to 300 °C and it consists of a hexacoordinated titanium center to which a chain of ethylene glycol ligands is chelated. This has been reported by Wang et al., albeit using a different synthetic methodology.[9] Moreover, we have determined that this pattern shows exclusively a preferential alignment along the (100) axis when compared to the simulated XRD pattern from the crystal structure.[9] It has been determined in our lab that for proper formation of the titanium glycolate precursor, complete hydrolysis of the titanium *n*-butoxide needs to occur along with removal of any water that might be present (see Supporting Information for further synthesis details).[14] Upon further heating, it was determined that pure anatase and rutile phases were formed at 500 and 800 °C, respectively. Figure 2 shows the representative SEM images. It can be observed that only rod-like morphology is observed, and the reason stems mainly from the unit cell arrangement: $C2/c$ monoclinic space group which consists of one-dimensional chains of edge-sharing $Ti^{IV}O_6$ octahedra along the *c* axis. The size of the titanium glycolate rods was determined to be $33.4 \pm 15.7\,\mu m$ in length and $2.9 \pm 0.9\,\mu m$ in width. After conversion to the anatase and rutile phases, the rod-like morphology was maintained (Figures 2c–2f). The dimensions of the anatase rods were 11.5 ± 2.3 and $0.9 \pm 0.2\,\mu m$, and the rutile rods were 13.5 ± 3.1 and $1.0 \pm 0.2\,\mu m$ in length and width, respectively. This clearly indicated that there was a substantial shrinkage of the rods upon heating. For the conversion to anatase, the decrease can be attributed to loss of the organic ligands. However, a slight increase in size was ob-

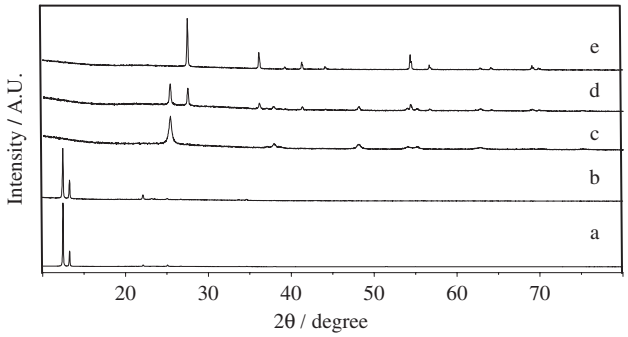

Figure 1. Powder XRD patterns of (a) as-synthesized titanium glycolate and after heating to (b) 300, (c) 500, (d) 700, and (e) 900 °C.

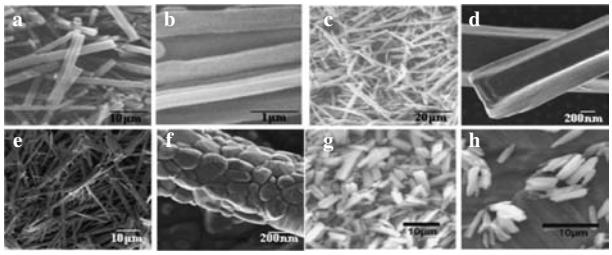

Figure 2. SEM micrographs of (a), (b) as-synthesized titanium glycolate, (c), (d) anatase, (e), (f) rutile, and (g) reflux temp 150 °C; reflux time 1 h (h) reflux temp 130 °C; reflux time 3 h.

served upon conversion from anatase to rutile. Anatase has a larger unit cell ($a = b = 3.78$ Å, $c = 9.51$ Å; unit cell volume per chemical formula (V/z where $z = 4$) is 34.0 Å^3; JCPDS File No. 04-006-9240) when compared to rutile ($a = b = 4.58$ Å, $c = 2.95$ Å; $V/z = 30.9$ Å^3; JCPDS File No. 01-071-6411). This growth can be attributed to an increase in the overall size of the rutile crystallites due to annealing. This concomitantly leads to improved crystallinity of the sample. It can also be observed that the Ti–glycolate and anatase rods both have smooth surfaces whereas for the rutile phase consists of coalesced crystallites. The average diameter of these crystallites was determined to be ca. 70–100 nm. It was also observed that the sizes of the rods could be tuned by altering the synthesis parameters. The smallest dimensions obtained were 3.4 ± 0.8 μm in length and 0.7 ± 0.2 μm in width (Figures 2g–2h) after refluxing for 1 h.

The samples were further characterized using TGA and FTIR spectroscopy.[14] TGA data indicated a two-step pattern for weight loss. The loss in the range of 25–200 °C was due to removal of physisorbed water and ethylene glycol, and the second in the range of 200–450 °C was attributed to removal of ligated ethylene glycol. FTIR studies of titanium glycolate displayed peaks at 1073 and 1225 cm^{-1} (stretching mode of alcohol C–O).[10] Bands were also observed at 1457 and 1654 cm^{-1} which were due to the O–H bending mode.[10] A broad peak in the region 3200–3500 cm^{-1} was due to physically adsorbed water and the hydrogen bonding involving ethylene glycol O–H groups, and a peak at 635 cm^{-1} was assigned to the Ti–O stretching mode.[10] After calcination, O–H and C–H bands were no longer prevalent, whereas the Ti–O stretching band was broadened. This corroborated with other measurements that the organic components were completely removed by heat treatment.

For the grafting of gold NPs, upon following method A, a minimal coverage was observed of Au onto TiO_2 surface. In order to obtain a better distribution, method B was followed. Figure 3 shows the TEM images of the materials prepared by this method. Moreover, the cetyltrimethylammonium bromide (CTAB) mesophase can be observed on the surface of Ti–glycolate rods, Figure 3a, within which Au NPs are embedded. Furthermore, a weight loss corresponding to CTAB moiety (ca. 37%) was observed in TGA which supports the interaction between Ti–glycolate rods and CTAB. This newly formed composite sample was converted to anatase and rutile after calcining at the required elevated temperatures. This led to concurrent removal of CTAB mesophase; however, importantly, the Au NPs were still prevalent after the heat treatment, Figures 3b and 3c. It is important to point out that even after calcinations at elevated temperatures, Au NPs could still be seen as individual structures and that they were uniformly distributed on the surface, albeit with a concomitant increase in size. Synthesized Au citrate-capped NPs were ca. 3.5 nm, upon aggregating them on to the titanium glycolate rods, the size increased to ca. 12.5 nm, and on anatase and rutile it was found to be ca. 40 and 32 nm, respectively. XRF measurements conclusively proved the presence of Au NPs (see Supporting Information for loading levels).[14]

In method B, self-assembled adsorption of CTAB onto the Ti–glycolate surface is the pivotal step. It is well known that depending on the concentration of the amphiphile, a variety of aggregated CTAB structures (e.g., hemimicelle, admicelle, and/or a bilayer) adsorb though electrostatic interactions onto the negative sites of the TiO_2 surface.[11] As the concentration used in our experiments is above the cmc, it is hypothesized that at least a uniform bilayer (or more) is present on the surface. Subsequently, Au NPs (citrate capped) are introduced. Since the affinity of CTAB is higher for Au surface,[12] the citrate ions are replaced while still maintaining NP integrity, and the Au NPs are easily embedded in the compatible mesophase. This procedure involves chemical interaction invovling hydrophobic forces to direct the assembly of the Au NPs onto the surface of the TiO_2 surface; hence, the loadings are dramatically higher than the control experiments where no CTAB was used. Subsequently, upon calcination, two events occur simulaneously: (1) anatase and rutile phases form (depending on the temperature) and (2) CTAB is removed, giving an oxide surface coated with Au NPs.[13]

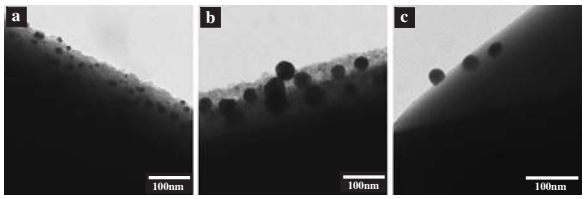

Figure 3. TEM images after assembling of Au NPs onto (a) CTAB-equilibrated Ti–glycolate rods and their conversion to (b) anatase and (c) rutile by method B.

In summary, the successful synthesis of rod-like TiO_2 has been presented. Also, a strategy has been developed to anchor Au NPs which can be extended to other NPs.

References and Notes

1 X. Chen, S. S. Mao, *Chem. Rev.* **2007**, *107*, 2891.
2 Y. Xia, P. Yang, Y. Sun, Y. Wu, B. Mayers, B. Gates, Y. Yin, F. Kim, H. Yan, *Adv. Mater.* **2003**, *15*, 353.
3 L. Kavan, M. Kalbac, M. Zukalova, I. Exnar, V. Lorenzen, R. Nesper, M. Grätzel, *Chem. Mater.* **2004**, *16*, 477.
4 S. Lee, C. Jeon, Y. Park, *Chem. Mater.* **2004**, *16*, 4292.
5 T. Peng, A. Hasegawa, J. Qiu, K. Hirao, *Chem. Mater.* **2003**, *15*, 2011.
6 L.-S. Zhong, J.-S. Hu, Z.-M. Cui, L.-J. Wan, W.-G. Song, *Chem. Mater.* **2007**, *19*, 4557.
7 E. György, G. Sauthier, A. Figueras, A. Giannoudakos, M. Kompitsas, I. N. Mihailescu, *J. Appl. Phys.* **2006**, *100*, 114302.
8 L.-S. Zhong, J.-S. Hu, Z.-M. Cui, L.-J. Wan, W.-G. Song, *Chem. Mater.* **2007**, *19*, 4557.
9 D. Wang, R. Yu, N. Kumada, N. Kinomura, *Chem. Mater.* **1999**, *11*, 2008.
10 A. D. Cross, *Introduction to Practical Infra Red Spectroscopy*, Butterworths, London, **1969**.
11 H. Li, C. P. Tripp, *Langmuir* **2002**, *18*, 9441.
12 B. D. Busbee, S. O. Obare, C. J. Murphy, *Adv. Mater.* **2003**, *15*, 414.
13 Y. S. Chaudhary, J. Ghatak, U. M. Bhatta, D. Khushalani, *J. Mater. Chem.* **2006**, *16*, 3619.
14 Supporting Information is available electronically on the CSJ-Journal Web site, http://www.csj.jp/journals/chem-lett/index.html.

Published on the web (Advance View) June 27, 2009; doi:10.1246/cl.2009.764